Structural coherence and layer perfection in Fe/MgO multilayers

2008 J. Phys.: Condens. Matter 20 055212

(http://iopscience.iop.org/0953-8984/20/5/055212)

J. Phys.: Condens. Matter **20** (2008) 055212 (5pp) doi:10.1088/0953-8984/20/5/055212

Structural coherence and layer perfection in Fe/MgO multilayers

Hossein Raanaei[1,2], Hans Lidbaum[3], Andreas Liebig[1], Klaus Leifer[3] and Björgvin Hjörvarsson[1]

[1] Department of Physics, Uppsala University, Box 530, 751 21 Uppsala, Sweden
[2] Department of Physics, Persian Gulf University, Boushehr 751 68, Iran
[3] Institute of Electron Microscopy and Nano-Engineering, Uppsala University, Box 534, SE 751 21, Sweden

E-mail: bjorgvin.hjorvarsson@fysik.uu.se

Received 14 September 2007, in final form 12 December 2007
Published 17 January 2008
Online at stacks.iop.org/JPhysCM/20/055212

Abstract
A series of Fe/MgO multilayers was grown on single-crystal MgO(001) substrates at different temperatures using magnetron sputtering. The structural quality of the samples was investigated by x-ray reflectometry, x-ray diffraction and transmission electron microscopy. The results show a strong dependence of the structural quality on the growth temperature. Although good epitaxial layers are obtained at 165 °C, the sample does not exhibit any superlattice diffraction peaks. This effect is shown to be related to a continuous variation of the distance between the Fe layers as well as between the MgO layers.

1. Introduction

The attempt to realize well defined magnetic/insulating layers has caused considerable research effort lately. This has to a large extent been attributed to increasing interest in tunnelling magnetoresistance (TMR) and related phenomena [1–3]. Epitaxially grown Fe(001)/MgO(001)/Fe(001) trilayers [4] can be considered as a model system in this context. Kanaji *et al* [5–7] performed the first epitaxial growth of body-centered cubic (bcc) Fe on MgO(001). They identified the Fe(001) [110]‖MgO(001) [100] epitaxial relation, resulting from a lattice match of MgO ($a = 4.213$ Å) and Fe ($a = 2.866$ Å) upon a 45° in-plane rotation. Several growth studies of Fe(001) on MgO(001) substrate have already been reported [8, 9], and epitaxial growth of MgO(001) and Fe/MgO/Fe(001) trilayer on Fe(001) substrate has been performed as well [10–12].

The interface quality in ultrathin layers and multilayered heterostructures plays an important role in the resulting physical properties. This includes the presence of interface magnetic anisotropy, transport as well as magneto-transport properties in tunnel junctions. It is therefore of interest to obtain an understanding of the growth parameters governing the resulting structures. Here we describe investigations of the influence of the growth temperature, allowing optimization of the layering and the crystallinity of Fe/MgO multilayers. We will demonstrate the feasibility of the growth of high-quality MgO/Fe multilayers and discuss the absence of high-angle diffraction peaks from the multilayer structure.

2. Experiment

Fe/MgO multilayers were grown using magnetron sputtering. The Fe layers were deposited from an Fe target (99.95%) using a dc source, while the MgO layers were deposited using an MgO target (99.9%) and rf sputtering. The Fe and MgO deposition rates were determined to be 0.35 and 0.05 Å s^{-1}, respectively, using x-ray reflectivity measurements from a calibration sample. The base pressure of the chamber was less than 5×10^{-9} Torr and the operating pressure of Ar gas, with a purity of 99.9999%, was kept at 2.0 mTorr. No additional oxygen was introduced in the chamber during growth. All the samples were grown on MgO(001) single-crystal substrates, which were annealed at 530 °C for 1 h prior to deposition. The multilayers consist of 15 repetitions of Fe/MgO bilayers, all starting with the growth of Fe on the MgO(001) substrates. All the samples were capped with 14 Å thick Al_2O_3 to prevent oxidation. A series of samples was grown at temperatures from 120 ± 10 to 290 ± 10 °C, keeping all other growth parameters identical.

Structural analysis was performed by both x-ray diffraction (XRD), x-ray reflectivity (XRR) and transmission electron microscopy (TEM). The XRD and XRR analyses were

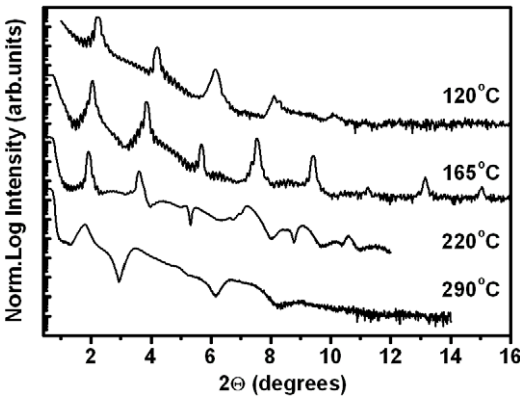

Figure 1. Low-angle reflectivity spectra of $[Fe/MgO]_{15}$ multilayer thin films at different growth temperatures. The number of repeats is 15 for all the samples, and the nominal thicknesses were the same. Scans are offset for clarity.

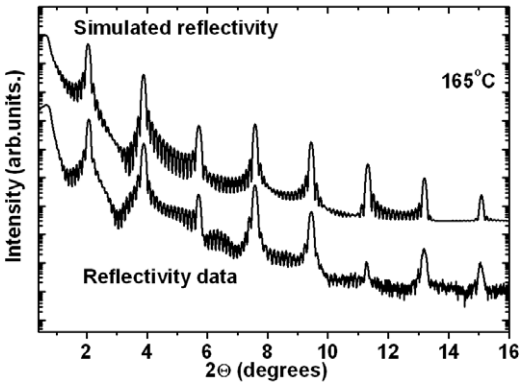

Figure 2. XRR with simulated reflectivity curve of sample grown at 165 °C is used to determine the bilayer thickness and interface widths. Graphs are offset for clarity.

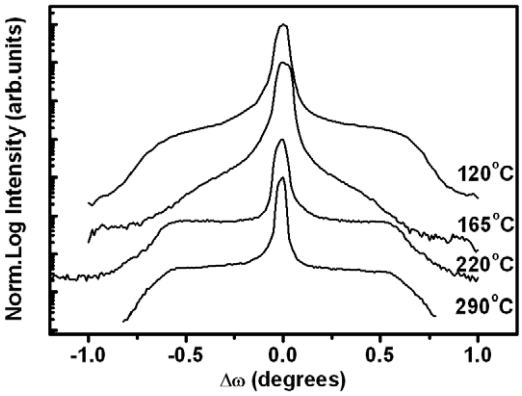

Figure 3. Rocking curves measured over the first-order reflectivity peak of each sample; see figure 1. Scans are offset for clarity.

performed using a Siemens D5000 diffractometer with Cu Kα ($\lambda = 1.5418$ Å) in a standard Bragg–Brentano geometry.

The TEM measurements were performed using an FEI Tecnai F30ST microscope operated at 300 kV. In the scanning transmission electron microscopy mode (STEM), we used a Fischione high-angle annular dark-field detector (HAADF). The cross-sectional (TEM) samples were prepared using a conventional cross-sectional sample preparation technique [13]. Propylene glycol (water content <0.1%) was used during preparation, as a water-based solvent often leads—probably by magnesium hydroxide formation—to cracks in the substrate. The samples were thinned to electron transparency by a grazing-incidence Ar ion beam in a Gatan PIPS (initially 3.5 keV and finally 1.9 keV).

3. Results and discussion

The chemical modulation was investigated using both XRR and TEM. The XRR results for all the samples are illustrated in figure 1. As seen in the figure, the low-temperature growth results in reasonably well defined reflectivity patterns, of which the sample grown at 165 °C shows the largest number of reflections and has the smallest width of the peaks. The total thickness oscillations are also most pronounced for this sample, indicating well defined layering at all relevant length scales. The decrease in the intensity of the higher-order reflections at the samples grown above or below 165 °C represent increasing variation in the thickness of the layers. The thickness variation also leads to a suppression of the total thickness oscillations, which have completely vanished at a growth temperature of 290 °C. Thus, from the XRR results, the optimal growth temperature appears to be around 165 °C.

The XRR results for the sample grown at 165 °C were simulated using the GenX program [14], and the results are shown in figure 2. The simulation yielded a bilayer thickness of $\Lambda = 47 \pm 1$ Å, an Fe thickness of $t_{Fe} = 32 \pm 0.5$ Å and an MgO thickness of $t_{MgO} = 15.2 \pm 0.5$ Å. The average interface width is 2–3 Å between the Fe and MgO. Thus the result is consistent with a variation in thickness corresponding to about ± 1 ML (monolayers) of Fe and MgO. The oxidation state of the Fe layers at the MgO interfaces [15–17] is undetermined here, which can affect the deduced interface width.

Figure 3 shows ω scans (rocking curves) at the first-order reflectivity peak for each sample. The ω scan reveals two components: one sharp and one much wider. The first component, whose width is mainly determined by the instrument resolution, corresponds to specular scattering. The second component is diffuse scattering and corresponds to imperfections in the layering [18, 19]. As seen in figure 3, the samples grown at the lowest temperatures exhibit decreasing intensity with increasing/decreasing $\Delta\omega$, while growth at the highest temperature yields a constant off-specular contribution in the whole accessible range. The largest intensity in the specular contribution is obtained for the sample grown at 165 °C, which also exhibits a steep decrease in off-specular scattering with increasing/decreasing $\Delta\omega$. These observations are consistent with the best layering of the sample grown at 165 °C, while higher as well as lower growth temperatures give rise to significantly more off-specular scattering. Thus, roughness/waviness is minimal in the sample grown at 165 °C.

Although the x-ray reflectivity results are conclusive with respect to the changes in quality of the layering, these do not yield unique information on the type of imperfections

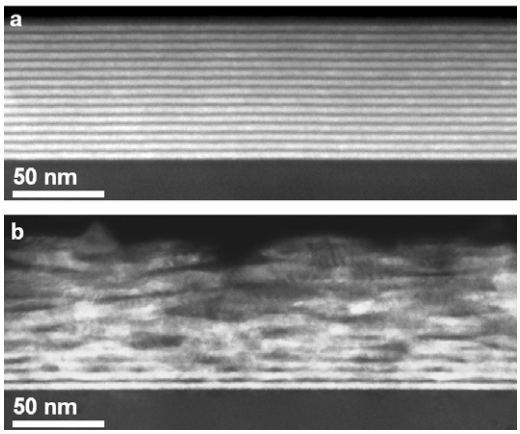

Figure 4. HAADF-STEM images of $[Fe/MgO]_{15}$ multilayers grown at two different growth temperatures. The sample grown at 165 °C shows a distinct modulation between the Fe (bright) and MgO (dark) layers on the MgO substrate, as seen in (a). In the sample grown at 290 °C the variation in the thickness of the layers is already altered strongly after the first two repetitions, as seen in (b).

resulting in the broadening observed in the x-ray reflectivity data. Furthermore, the mechanism for the decay of the layering, which is apparent at the highest temperatures, is not obtainable. To obtain real-space information on these changes with growth temperature, we acquired HAADF-STEM images, which provides Z-contrast of the layered structure. The results are illustrated in figure 4, showing continuous layers with very small thickness variation/roughness of the sample grown at 165 °C. No cumulative roughness is apparent and the layering is close to perfect at the length scales that were probed.

The results obtained for the sample grown at 290 °C are in strong contrast to the results for the sample grown at 165 °C. The layers are initially reasonably well defined in the sample grown at 290 °C, but the second layer already exhibits a significant thickness variation and a strong increase in the waviness is observed with increasing distance from the substrate. The apparent variation in layer thickness can be viewed as a cumulative roughness which is only weakly correlated. Thus, the TEM results support the interpretation of the x-ray reflectivity data and yield a clear real-space picture of the underlying reason for the lack of well defined reflectivity peaks for the samples grown at the highest temperatures. Furthermore, the origin of the difference in the reflectivity data is easily understood from these images. The well defined layering should give rise to larger and better defined reflectivity peaks, as is apparent from the data discussed above. Thus, the perfection of the layers strongly depends on the growth temperature, and we conclude the growth at 165 °C to yield the smallest variation in the thickness of the layers.

Let us now consider the crystallinity, as viewed from the XRD analysis. First of all, a wide scan in the high-angle region exhibited the complete absence of superlattice peaks, even for the sample grown at 165 °C. Two features were observed, firstly a well defined peak corresponding to the (002) diffraction from the MgO substrate, and secondly a wide peak at around 65° corresponding to Fe(002), as illustrated in figure 5.

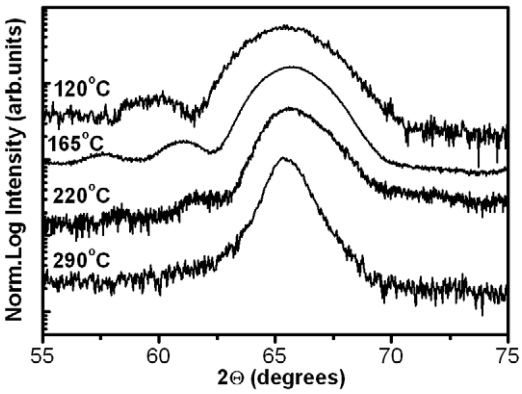

Figure 5. XRD scans of samples at different temperatures show the Bragg peaks for each sample at about 65° (iron bulk peak). There are no superlattice peaks in the scan.

The 2Θ position of the Fe(002) peak for samples with growth temperatures of 120, 165 and 220 °C are 65.68°, 65.70° and 65.71°, respectively. The 2Θ position of bulk iron corresponds to 65.1°. The increasing shift of the (002) reflection toward higher angles reflects the decreasing lattice spacing of Fe (1.4299, 1.4195 and 1.4193 Å) perpendicular to the layers with increasing growth temperature. The decrease in lattice spacing originates in an elastic response from the increasing in-plane lattice parameter [20], resulting in changes in the tetragonal distortion of the Fe lattice. The peak position of Fe(002) for a sample grown at 290 °C is 65.32°, which corresponds to the 2Θ position for bulk iron, thereby indicating that such iron layers are almost fully relaxed.

Well defined Laue oscillations are observed for the sample grown at 165 °C. These oscillations correspond to an Fe thickness of 26 Å, which is consistent with the nominal thickness of the Fe layers as well as the simulations of the x-ray reflectivity data. Thus, we can conclude that the Fe layers are acting as independent scatterers.

The other samples do not exhibit such clear oscillations, consistent with larger variations in the Fe layer thickness in these samples. These features can be understood by independent scattering from the Fe layers. The Fe(002) peak can therefore be viewed as a sum of scattering from 15 independent Fe layers. This picture is consistent with the absence of superlattice peaks, and the underlying reason is discussed below. The sample grown at the highest temperature does not exhibit any total thickness oscillations at all, although the full width at half maximum of the peak is the smallest. This apparent contradiction is resolved when considering the influence of the variation in thickness on the width of the Bragg peak. As seen in figure 4, there is a substantial variation in the thickness of the layers. Therefore, there are regions with both significantly smaller and larger thicknesses compared to the mean value. When scattering from these regions is independent, the resulting width of the Fe(002) peak in 2Θ reflects the volume fraction of the regions with different thicknesses. The width of the Bragg peak can also be used to estimate the out-of-plane coherence length. The coherence length of the sample grown at 165 °C is determined to be on the order of 30 Å using the Scherrer equation [21], which

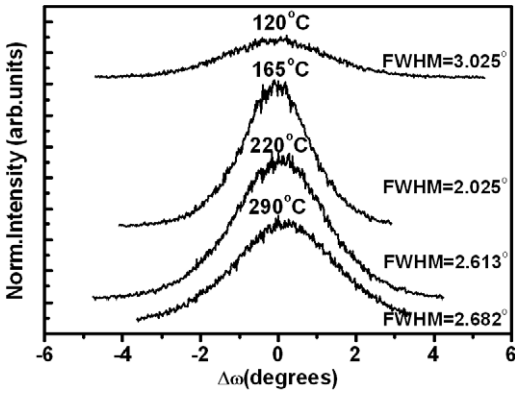

Figure 6. Rocking curves measured around the Fe(002) Bragg peak of each sample show the lowest mosaicity for the sample grown at 165 °C. Scans are offset for clarity.

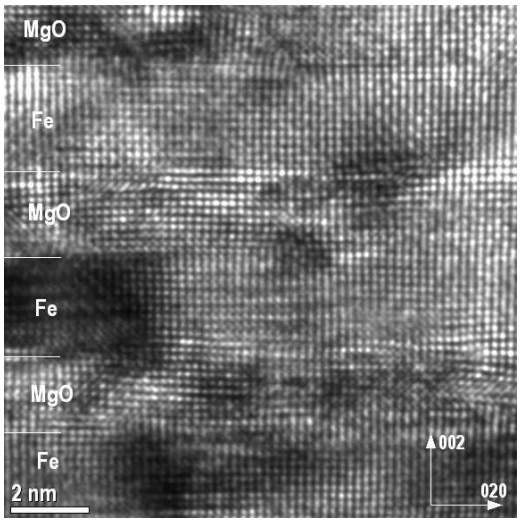

Figure 7. High-resolution phase contrast TEM micrograph of the Fe/MgO multilayer grown at 165 °C. Only small variations in the thickness of layers are observed. The image confirms a bilayer thickness of ≈48 Å, with individual layer thicknesses of ≈20 Å MgO and ≈28 Å Fe. The orientation of the MgO substrate is indicated.

corresponds approximately to the thickness of the Fe layers in the sample. The width of the Fe(002) peak can therefore be concluded to reflect approximately the crystal coherency within a single Fe layer.

To obtain a better understanding of the crystalline structure, we performed rocking curve measurements on the Fe(002) peak, and the results are illustrated in figure 6. As seen in the figure, the smallest width is obtained for the sample grown at 165 °C, consistent with best crystalline quality of that sample. The lowest degree of crystallinity is obtained for the sample grown at the lowest temperature. Thus, although the layering is reasonable when growing the samples at 120 °C, the crystallinity is not.

To explore the crystallinity and the epitaxial relations of the layers further, we performed high-resolution TEM analysis of the sample grown at 165 °C. The results are shown in figure 7. The apparent shading in the micrograph is caused by variations in the orientation of the crystal planes, consistent with the high density of small-angle grain boundaries. Throughout each of the Fe and MgO layers, the Fe(002) and MgO(002) lattice planes appear to be in registry with each other. When the Fe(110) and MgO(100) planes (orthogonal to the layers) are observed, they also appear to be in registry to each other. Since the layers appear to be coherent and in registry with each other, the absence of superlattice diffraction peaks is quite surprising; see figure 5. Up to eight superlattice diffraction peaks are expected within the 2Θ range 55°–75°. To understand this apparent contradiction, we need to explore the apparent imperfections in the structure. First of all, the Fe and the MgO layers grow with a 45° rotation of the [100] crystallographic directions of the constituents $[110]_{Fe}\|[100]_{MgO}$ [5]. This rotation arises from the difference between the lattice parameters of Fe and MgO, which are 2.86 and 4.21 Å respectively, allowing close to epitaxial growth of the layers.

However, the growth of the layers is not phase locked. This implies the presence of incomplete MgO layers, on which the Fe layers must grow. The step height of the MgO terraces is close to 2.1 Å, which is much larger than the equivalent thickness of one monolayer of Fe (1.43 Å). The same holds for the growth of MgO on Fe underlayers with a step height of about 1.43 Å. Hence, the presence of atomic steps and terraces will inevitably result in a continuous variation in the distance between atomic planes in, for example, neighbouring Fe layers, as $(d_{MgO}–d_{Fe}) \simeq (\sqrt{2}-1)d_{Fe}$. This incompatible difference in atomic distances cannot be taken up by any rotation, as for the in-plane adaption of the layers. The difference in the distance of the atomic planes will therefore give rise to large local strain fields at the edges of the terraces, which in turn can act as a driving force for the increased waviness at elevated temperatures. Such strain fields can equally act as a source for inclinations of lattice planes, leading to a broadening of several degrees in the rocking curve. For the sample grown at 165 °C we observe no waviness, still superlattice reflections are absent in the region of the Fe(002) peak. At the same time, we observe inclinations of the in-plane lattice planes of 0°–4° in the high-resolution images such as that shown in figure 7. This is in agreement with the peak width observed in the rocking curve illustrated in figure 6.

The absence of superlattice peaks can therefore be understood by considering the continuous variation in the distance of the Fe–Fe and the MgO–MgO layers, caused by the incompatible (001) lattice distances of the constituents. Thus the scattering from each layer in the superlattice is independent of the rest of the sample. This interpretation is supported by the work of Clemens *et al* [22], which demonstrated the absence of superlattice peaks in superlattices with a continuous variation in the distance between the layers. The absence of superlattice peaks was shown to require continuous variation of the distance between the layers corresponding to one to two monolayers, similarly to the inferred variation in the Fe/MgO multilayers discussed here. Both the Fe and MgO layers will therefore scatter independently in the high-angle region, due to the phase shift caused by the incompatible lattice distances at the edges of the terraces. Interestingly, Clemens *et al* [22] also showed that superlattice reflections in the high-angle region

are still obtained with a discrete roughness of even several monolayers. This qualitative interpretation of the influence of the incompatible height variation of the terraces on the intensity brings new insight to the nature of these multilayers. Thus, the observation of the very good layer stacking sequence is in good agreement with the presence of continuous and uncorrelated variation in the layer thickness.

4. Conclusion

In this work, the influence of the growth temperature on the chemical modulation and crystallinity of Fe/MgO multilayers has been studied. Although there is considerable strain in the layers, we still demonstrate layer growth with a high degree of planarity. The growth temperature has a strong influence on the resulting sample quality, and good crystal structure is obtained for a growth temperature of 165 °C. The variation in the layer thickness is shown to be uncorrelated, which in turn leads to the absence of layer undulations and cusps at this growth temperature.

Acknowledgments

The authors would like to acknowledge the Swedish Research Council (VR), the Swedish Foundation for Strategic Research (SSF), and the Wallenberg Foundation for financial support, and Ernesto Coronel for his help and fruitful discussions.

References

[1] Miyazaki T and Tezuka N 1995 Giant magnetic tunneling effect in Fe/Al_2O_3/Fe junction *J. Magn. Magn. Mater.* **139** (3)
[2] Moodera J S and Kinder L R 1996 Ferromagnetic–insulator–ferromagnetic tunneling: spin-dependent tunneling and large magnetoresistance in trilayer junctions (invited) *J. Appl. Phys.* **79** 4724–9
[3] Moodera J S, Kinder L R, Wong T M and Meservey R 1995 Large magnetoresistance at room temperature in ferromagnetic thin film tunnel junctions *Phys. Rev. Lett.* **74** 3273–6
[4] Yuasa S, Nagahama T, Fukushima A, Suzuki Y and Ando K 2004 Giant room-temperature magnetoresistance in single-crystal Fe/MgO/Fe magnetic tunnel junctions *Nat. Mater.* **3** 868–71
[5] Kanaji T, Asano K and Nagata S 1973 Behaviour of impurity atoms and adsorbed O atoms on (001) face of Fe epitaxial film *Vacuum* **23** 55–9
[6] Kanaji T, Kagotani T and Nagata S 1976 Auger and loss-spectroscopy study of surface contamination effect on the growth mode of Fe epitaxial films on MgO(001) *Thin Solid Films* **32** 217–9
[7] Urano T and Kanaji T 1988 Atomic and electronic structure of ultrathin iron film on MgO(001) surface *J. Phys. Soc. Japan* **57** 3403–10
[8] Jordan S M, Lawler J F, Schad R and van Kempen H 1998 Growth temperature dependence of the magnetic and structural properties of epitaxial Fe layers on MgO(001) *J. Appl. Phys.* **84** 1499–503
[9] Lawler J F, Schad R, Jordan S and Van Kempen H 1997 Structure of epitaxial Fe films on MgO (100) *J. Magn. Magn. Mater.* **165** 224–6
[10] Dynna M, Vassent J L, Marty A and Gilles B 1996 A low-energy electron diffraction investigation of the surface deformation induced by misfit dislocations in thin MgO films grown on Fe (001) *J. Appl. Phys.* **80** 2650–7
[11] Vassent J L, Dynna M, Marty A, Gilles B and Patrat G 1996 A study of growth and the relaxation of elastic strain in MgO on Fe(001) *J. Appl. Phys.* **80** 5727–35
[12] Wulfhekel W, Klaua M, Ullmann D, Zavaliche F, Kirschner J, Urban R, Monchesky T and Heinrich B 2001 Single-crystal magnetotunnel junctions *Appl. Phys. Lett.* **78** 509
[13] Alani R and Swann P R 1992 Precision ion polishing—a new instrument for TEM specimen preparation of materials *Specimen Prep.-III* vol 254, ed R Anderson, B Tracy and J Bravmann (Pittsburgh: MRS)
[14] Björck M and Andersson G 2007 Genx: an extensible x-ray reflectivity refinement program utilizing differential evolution *J. Appl. Crystallogr.* **40** 1174–8
[15] Palomares F J, Munuera C, Boubeta C M and Cebollada A 2005 Spatial and chemical interface asymmetry in Fe/MgO/Fe (001) heterostructures *J. Appl. Phys.* **97** 036104
[16] Meyerheim H L, Popescu R, Jedrecy N, Vedpathak M, Sauvage-Simkin M, Pinchaux R, Heinrich B and Kirschner J 2002 Surface x-ray diffraction analysis of the MgO/Fe (001) interface: evidence for an FeO layer *Phys. Rev.* B **65** 144433
[17] Meyerheim H L, Popescu R, Kirschner J, Jedrecy N, Sauvage-Simkin M, Heinrich B and Pinchaux R 2001 Geometrical and compositional structure at metal–oxide interfaces: MgO on Fe (001) *Phys. Rev. Lett.* **87** 76102
[18] Savage D E *et al* 1991 Determination of roughness correlations in multilayer films for x-ray mirrors *J. Appl. Phys.* **69** 1411
[19] Zabel H 1994 X-ray and neutron reflectivity analysis of thin films and superlattices *Appl. Phys.* A **58** 159–68
[20] Moons R, Blässer S, Dekoster J, Vantomme A, De Wachter J and Langouche G 1998 Structural characterization of thin epitaxial Fe films *Thin Solid Films* **324** 129–33
[21] Warren B E 1990 *X-Ray Diffraction* (New York: Dover)
[22] Clemens B M and Gay J G 1987 Effect of layer-thickness fluctuations on superlattice diffraction *Phys. Rev.* B **35** 9337–40